EMOTION ESTIMATION VIA TENSOR-BASED SUPERVISED DECISION-LEVEL FUSION FROM MULTIPLE BRODMANN AREAS

Kento Sugata[†], *Takahiro Ogawa*[†] *and Miki Haseyama*[‡] [*]

[†‡]Graduate School of Information Science and Technology, Hokkaido University
N-14, W-9, Kita-ku, Sapporo, Hokkaido, 060-0814, Japan
E-mail: [†] {sugata,ogawa}@lmd.ist.hokudai.ac.jp, [‡]miki@ist.hokudai.ac.jp

ABSTRACT

This paper presents a novel method that estimates human emotion based on tensor-based supervised decision-level fusion (TS-DLF) from multiple Brodmann areas (BAs). From multiple brain data corresponding to these BAs captured by functional magnetic resonance imaging (fMRI), our method performs general tensor discriminant analysis (GTDA) to obtain features which can reflect the user's emotion. Furthermore, since the dimension of the obtained features becomes lower, this can avoid overfitting in the following training procedure of estimators. Next, by separately using the transformed BA data obtained after GTDA, we obtain multiple estimation results of the user's emotion based on logistic tensor regression (LTR). Then our method realizes the decision of the final result based on TS-DLF from the multiple estimation results. This approach, *i.e.,* the integration of the multiple BAs' results for the whole-brain data, is the biggest contribution of this paper. TS-DLF successfully integrates the multiple estimation results with considering the performance of the LTR-based estimator constructed for each BA. Experimental results show that our method outperforms *state-of-the-art* approaches, and the effectiveness of our method can be confirmed.

Index Terms— Emotion estimation, functional magnetic resonance imaging, tensor dimensionality reduction, tensor decision-level fusion

1. INTRODUCTION

Affect (*e.g.,* moods or emotions) is the core of human nature and behavior [1]. In the field of "affective computing" [2], studies on estimation of moods or emotions from neuropsychological signals such as functional magnetic resonance imaging (fMRI) data have been intensively carried out. Furthermore, in recent years, machine learning techniques have been increasingly used in the analysis of fMRI data while users are watching images [3–6]. Generally, the small sample size problem occurs in fMRI data analysis [6–8], *i.e.,* the dimensionality of whole-brain data is generally larger than the number of observations. Typically, this problem results in overfitting of training data, leading to high classification accuracy for the data used in designing the classifier, but poor classification accuracy for test data.

This paper presents a novel method for estimating human emotion evoked by visual stimuli using fMRI data. In order to solve the above problem, we perform division of the whole-brain data according to the Brodmann areas (BAs) [9]. Each area is a region of the cerebral cortex, and the BAs were originally defined and numbered by Brodmann based on cytoarchitecture. In our method, general tensor discriminant analysis (GTDA) [10] is applied to the data obtained from each BA (BA data). GTDA takes the information related to users' emotion into account and deals with tensor objects such as fMRI data to provide the corresponding lower-dimensional tensor for avoiding the risk of the overfitting. Next, we obtain a logistic tensor regression (LTR) [11]-based estimation result for each BA. Since LTR can keep the intrinsic structural information in tensor objects, it outperforms vector-based approaches such as support vector machine (SVM) [12]. Finally, we integrate the LTR-based estimation results based on tensor-based supervised decision-level fusion (TS-DLF), which can be derived by collaboratively using LTR and the DLF proposed in [13]. The derivation of TS-DLF and the integration of the multiple BAs' estimation results for the whole-brain data are the biggest contribution of this paper. The TS-DLF successfully integrates the estimation results considering the accuracy of each LTR-based estimator. Consequently, the above nonconventional fMRI data analysis realizes accurate emotion estimation and outperforms *state-of-the-art* approaches.

[*]This work was partly supported by JSPS KAKENHI Grant Number JP25280036.

2. NOTATIONS AND BASIC TENSOR ALGEBRA

This section shows notations and basic tensor algebra as preliminaries since our method deals with tensor objects, *i.e.,* fMRI data. In this paper, vectors (1-order tensors) are denoted by lowercase boldface letters, *e.g.,* $\mathbf{x}$, matrices (2-order tensors) by uppercase boldface letters, *e.g.,* $\mathbf{X}$, and tensors (3-order or higher) by calligraphic letters, *e.g.,* $\mathcal{X}$. For instance, a K-order tensor is denoted as $\mathcal{X} \in \mathbb{R}^{D^{(1)} \times D^{(2)} \times \cdots \times D^{(K)}}$, and it is addressed by K indices $d^{(k)} (k = 1, 2, \ldots, K)$.

The k-mode product of a tensor $\mathcal{X}$ by a matrix $\mathbf{U} \in \mathbb{R}^{P \times D^{(k)}}$ is denoted by $\mathcal{X} \times_k \mathbf{U} \in \mathbb{R}^{D^{(1)} \times D^{(2)} \times \cdots \times P \times \cdots \times D^{(K)}}$.

The inner product is denoted by

$$\langle \mathcal{X}, \mathcal{Y} \rangle = \mathrm{vec}(\mathcal{X})^\top \mathrm{vec}(\mathcal{Y}), \tag{1}$$

where the size of $\mathcal{Y}$ is the same as that of $\mathcal{X}$, and $\mathrm{vec}(\cdot)$ represents the vectorization operator. From the unfolded tensor equivalents, Eq. (1) can be rewritten as follows:

$$\langle \mathcal{X}, \mathcal{Y} \rangle = \mathrm{tr}(\mathbf{X}^{(k)} \mathbf{Y}^{(k)\top}), \tag{2}$$

where $\mathbf{X}^{(k)} \in \mathbb{R}^{D^{(k)} \times (D^{(1)} \cdots D^{(k-1)} D^{(k+1)} \cdots D^{(K)})}$ is the k-mode matricization of $\mathcal{X}$.

The Khatri-Rao (KR) product [14] of two matrices $\mathbf{X} \in \mathbb{R}^{D^{\mathbf{X}} \times I}$

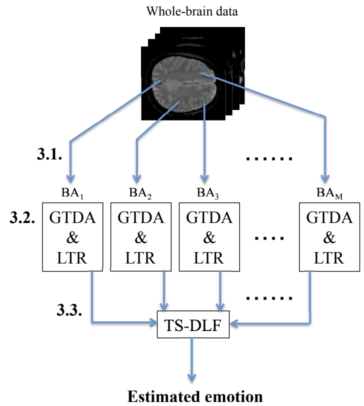

Fig. 1. The brief overview of our method.

and $\mathbf{Y} \in \mathbb{R}^{D^{\mathbf{Y}} \times I}$, $\mathbf{X} \odot \mathbf{Y} \in \mathbb{R}^{D^{\mathbf{X}} D^{\mathbf{Y}} \times I}$, is denoted as

$$\mathbf{X} \odot \mathbf{Y} = \begin{bmatrix} \mathbf{X}_{1,1}\mathbf{Y}_{:,1} & \mathbf{X}_{1,2}\mathbf{Y}_{:,2} & \dots & \mathbf{X}_{1,I}\mathbf{Y}_{:,I} \\ \mathbf{X}_{2,1}\mathbf{Y}_{:,1} & \mathbf{X}_{2,2}\mathbf{Y}_{:,2} & \dots & \mathbf{X}_{2,I}\mathbf{Y}_{:,I} \\ \vdots & \vdots & \ddots & \vdots \\ \mathbf{X}_{D^{\mathbf{X}},1}\mathbf{Y}_{:,1} & \mathbf{X}_{D^{\mathbf{X}},2}\mathbf{Y}_{:,2} & \dots & \mathbf{X}_{D^{\mathbf{X}},I}\mathbf{Y}_{:,I} \end{bmatrix},$$

where ":" represents the full range of the corresponding index.

The CANDECOMP/PARAFAC (CP) decomposition [15, 16] factorizes a K-order tensor $\mathcal{X}$ into a sum of R rank-one tensors as follows:

$$\mathcal{X} \approx \sum_{r=1}^{R} \mathbf{v}_r^{(1)} \circ \mathbf{v}_r^{(2)} \circ \dots \circ \mathbf{v}_r^{(K)},$$

where the operator "$\circ$" represents outer product, and the factor matrices are defined as $\mathbf{V}^{(k)} = [\mathbf{v}_1^{(k)}, \mathbf{v}_2^{(k)}, \dots, \mathbf{v}_R^{(k)}] \in \mathbb{R}^{D^{(k)} \times R}$. From unfolded tensors, the CP decomposition can be defined as

$$\begin{aligned} \mathbf{X}^{(k)} &= \mathbf{V}^{(k)} (\mathbf{V}^{(K)} \odot \dots \odot \mathbf{V}^{(k+1)} \odot \mathbf{V}^{(k-1)} \odot \dots \odot \mathbf{V}^{(1)})^\top \\ &= \mathbf{V}^{(k)} \mathbf{V}^{(-k)\top}, \end{aligned} \tag{3}$$

where $\mathbf{V}^{(-k)} = \mathbf{V}^{(K)} \odot \dots \odot \mathbf{V}^{(k+1)} \odot \mathbf{V}^{(k-1)} \odot \dots \odot \mathbf{V}^{(1)} \in \mathbb{R}^{\prod_{j=1, j \neq k}^{K} D^{(j)} \times R}$.

3. TENSOR-BASED EMOTION ESTIMATION METHOD FROM FMRI DATA

This section presents the proposed method that estimates human emotion evoked by visual stimuli using fMRI data. The brief overview of our method is shown in Fig. 1. Section **3.1** presents preprocessing and masking procedures to obtain the multiple BA data. In Sec. **3.2**, we apply GTDA to the BA data and perform LTR-based emotion estimation using the transformed BA data obtained after GTDA. We then integrate the LTR-based estimation results considering their estimation accuracies based on TS-DLF in Sec. **3.3**.

3.1. Preprocessing and Masking

This subsection presents the preprocessing and the masking procedures applied to the whole-brain data captured by an MRI equipment while users are watching images. Specifically, we adopt statistical parametric mapping[1] and wake forest university pick atlas [17, 18] as the preprocessing and the masking procedures, respectively. Since these procedures are not the main contribution of this paper, we only show their brief explanation, below.

The preprocessing procedure consists of the following three stages: realignment, spatial normalization and spatial smoothing [19]. Realignment corrected target images for the translational and rotational movements of the head. Next, in the spatial normalization, each scan is matched to the template, called Montreal neurological institute coordinates. Finally, the images were smoothed with a Gaussian filter of $8 \times 8 \times 8$ mm^3.

The masking procedure consists of the following two stages: generation of masks and calculation of the multiple BA data. In our method, we generate the multiple masks corresponding to BAs and take the product of the preprocessed whole-brain data by each mask to obtain the BA data [17, 18].

3.2. Single BA-based Emotion Estimation

Given a set of the training data of mth BA $\mathcal{X}_{i,m} \in \mathbb{R}^{D_m^{(1)} \times D_m^{(2)} \times D_m^{(3)}}$ ($i = 1, 2, \dots, N$, $m = 1, 2, \dots, M$; N and M being the number of the training data and the number of BAs, respectively), GTDA defines a multilinear transformation $\hat{\mathbf{U}}_m^{(k)} \in \mathbb{R}^{D_m^{(k)} \times P_m^{(k)}}$ ($P_m^{(k)} \leq D_m^{(k)}$, $k = 1, 2, 3$) that maps the original tensor space onto a lower-dimensional tensor subspace $\mathbb{R}^{P_m^{(1)} \times P_m^{(2)} \times P_m^{(3)}}$ as

$$\hat{\mathcal{X}}_{i,m} = \mathcal{X}_{i,m} \times_1 \hat{\mathbf{U}}_m^{(1)} \times_2 \hat{\mathbf{U}}_m^{(2)} \times_3 \hat{\mathbf{U}}_m^{(3)}.$$

Given the class labels of user's emotion $c_i \in \{0, 1\}$ corresponding to "positive" ($c_i = 1$) and "negative" ($c_i = 0$), k-mode between-class scatter matrix $\mathbf{S}_{B,m}^{(k)}$ and within-class scatter matrix $\mathbf{S}_{W,m}^{(k)}$ are calculated as follows:

$$\mathbf{S}_{B,m}^{(k)} = \sum_{c \in \{0,1\}} N_c (\bar{\mathbf{X}}_{c,m}^{(k)} - \bar{\mathbf{X}}_m^{(k)})(\bar{\mathbf{X}}_{c,m}^{(k)} - \bar{\mathbf{X}}_m^{(k)})^\top,$$

$$\mathbf{S}_{W,m}^{(k)} = \sum_{i=1}^{N} (\mathbf{X}_{i,m}^{(k)} - \bar{\mathbf{X}}_{c_i,m}^{(k)})(\mathbf{X}_{i,m}^{(k)} - \bar{\mathbf{X}}_{c_i,m}^{(k)})^\top,$$

where

$$\bar{\mathbf{X}}_{c,m}^{(k)} = \frac{1}{N_c} \sum_{\forall c_i = c} \mathbf{X}_{i,m}^{(k)},$$

$$\bar{\mathbf{X}}_m^{(k)} = \frac{1}{N} \sum_{i=1}^{N} \mathbf{X}_{i,m}^{(k)},$$

and N_c is the number of the training data belonging to cth class. The objective function of GTDA is defined as follows:

$$\hat{\mathbf{U}}_m^{(k)} = \arg\max_{\mathbf{U}_m^{(k)}} \ \mathrm{tr}\left(\mathbf{U}_m^{(k)\top} (\mathbf{S}_{B,m}^{(k)} - \zeta_m^{(k)} \mathbf{S}_{W,m}^{(k)}) \mathbf{U}_m^{(k)} \right),$$

where $\zeta_m^{(k)}$ equals to the maximum eigenvalue of $(\mathbf{S}_{W,m}^{(k)})^{-1} \mathbf{S}_{B,m}^{(k)}$. Let $\mathcal{X}_{test,m} \in \mathbb{R}^{D_m^{(1)} \times D_m^{(2)} \times D_m^{(3)}}$ be a test data of mth BA. The lower-dimensional tensor $\hat{\mathcal{X}}_{test,m} \in \mathbb{R}^{P_m^{(1)} \times P_m^{(2)} \times P_m^{(3)}}$ is obtained by

$$\hat{\mathcal{X}}_{test,m} = \mathcal{X}_{test,m} \times_1 \hat{\mathbf{U}}_m^{(1)} \times_2 \hat{\mathbf{U}}_m^{(2)} \times_3 \hat{\mathbf{U}}_m^{(3)}.$$

Next, we explain the LTR-based emotion estimation using single BA. The LTR model used in our method is shown in the following

[1] http://www.fil.ion.ucl.ac.uk/spm/

equation:

$$\Pr[c = 1|\hat{\mathcal{X}}_{test,m}, \mathcal{W}_m] = \frac{1}{1 + \exp(-\langle \mathcal{W}_m, \hat{\mathcal{X}}_{test,m}\rangle)},$$

where $\mathcal{W}_m \in \mathbb{R}^{P_m^{(1)} \times P_m^{(2)} \times P_m^{(3)}}$ is a parameter tensor of regression coefficients. For obtaining the optimal solution $\hat{\mathcal{W}}_m$ of $\mathcal{W}_m$, the following maximum log-likelihood problem is solved:

$$\hat{\mathcal{W}}_m = \arg\max_{\mathcal{W}_m} \mathcal{L}(\mathcal{W}_m),$$

where $\mathcal{L}(\mathcal{W}_m)$ is the log-likelihood function with respect to mth BA and defined as

$$\mathcal{L}(\mathcal{W}_m) = \sum_{i=1}^{N} \{c_i \ln\langle \mathcal{W}_m, \hat{\mathcal{X}}_{i,m}\rangle + (1 - c_i)\ln(1 - \langle \mathcal{W}_m, \hat{\mathcal{X}}_{i,m}\rangle)\}.$$

Since the regression coefficients $\mathcal{W}_m$ are constrained to be a sum of R rank-one tensors by using CP decomposition, $\mathcal{L}(\mathcal{W}_m)$ is rewritten as follows:

$$\mathcal{L}(\mathcal{W}_m) = \mathcal{L}(\{\mathbf{U}_m^{(1)}, \mathbf{U}_m^{(2)}, \mathbf{U}_m^{(3)}\}).$$

The above optimization problem can be solved by a coordinate descend approach of alternative projections in an iteration manner. Concretely, we solve the parameter $\mathbf{U}_m^{(k)}$ at each iteration, while keeping the other parameters $\{\mathbf{U}_m^{(j)}\}_{j=1, j\neq k}^{3}$ fixed. From Eqs. (2) and (3), we can obtain $\hat{\mathbf{U}}_m^{(k)}$ which maximizes

$$\begin{aligned}\mathcal{L}^{(k)}(\mathbf{U}_m^{(k)}) = &\sum_{i=1}^{N} c_i \ln\left(\mathrm{tr}(\mathbf{U}_m^{(k)} \mathbf{U}_m^{(-k)\top} \mathbf{X}_{i,m}^{(k)\top})\right) \\ &+ (1 - c_i)\ln\left(1 - \mathrm{tr}(\mathbf{U}_m^{(k)} \mathbf{U}_m^{(-k)\top} \mathbf{X}_{i,m}^{(k)\top})\right).\end{aligned}$$

Note that $\tilde{\mathbf{X}}_{i,m}^{(k)}$ is $\mathbf{X}_{i,m}^{(k)} \mathbf{U}_m^{(-k)}$, and $\mathrm{tr}(\mathbf{U}_m^{(k)} \mathbf{U}_m^{(-k)\top} \mathbf{X}_{i,m}^{(k)\top})$ is equal to the inner product of $\mathbf{U}_m^{(k)}$ and $\tilde{\mathbf{X}}_{i,m}^{(k)}$. Thus, since the following relationship holds:

$$\mathrm{tr}(\mathbf{U}_m^{(k)} \tilde{\mathbf{X}}_{i,m}^{(k)\top}) = \mathrm{vec}(\mathbf{U}_m^{(k)})^\top \mathrm{vec}(\tilde{\mathbf{X}}_{i,m}^{(k)}),$$

we can vectorize the problem as

$$\begin{aligned}\mathcal{L}^{(k)}\left(\mathrm{vec}(\mathbf{U}_m^{(k)})\right) = &\sum_{i=1}^{N} c_i \ln\left(\mathrm{vec}(\mathbf{U}_m^{(k)})^\top \mathrm{vec}(\tilde{\mathbf{X}}_{i,m}^{(k)})\right) \\ &+ (1 - c_i)\ln\left(1 - \mathrm{vec}(\mathbf{U}_m^{(k)})^\top \mathrm{vec}(\tilde{\mathbf{X}}_{i,m}^{(k)})\right).\end{aligned}$$

Finally, based on the idea of [11], we also add a regularization term and estimate the optimal solution as

$$\mathrm{vec}(\hat{\mathbf{U}}_m^{(k)}) = \arg\max_{\mathrm{vec}(\mathbf{U}_m^{(k)})} \mathcal{L}^{(k)}\left(\mathrm{vec}(\mathbf{U}_m^{(k)})\right) - \lambda \|\mathrm{vec}(\mathbf{U}_m^{(k)})\|_1,$$

where $\lambda > 0$ is a tuning parameter, and $\|\cdot\|_1$ represents L_1-norm. Consequently, we obtain the estimation result $y_{test,m}$ of human emotion for mth BA following below:

$$y_{test,m} = \arg\max_{c\in\{0,1\}} \Pr[c|\hat{\mathcal{X}}_{test,m}, \hat{\mathcal{W}}_m].$$

In this way, we can estimate the class of user's emotion. The problem, *i.e.,* the overfitting problem, is reduced by dividing the whole-brain data into multiple BA data (Sec. **3.1**) and the tensor-based BA data analysis approach shown in this subsection.

3.3. Integration of Multiple Estimation Results via TS-DLF

In this subsection, we newly derive TS-DLF to integrate the multiple estimation results obtained from each BA data. First, the estimation model, *i.e.,* the discriminating function, is specifically written as follows:

$$\Pr[c = 1|\hat{\mathcal{X}}_{test}, \mathcal{W}^{\mathrm{DLF}}] = \frac{1}{1 + \exp(-\langle \mathcal{W}^{\mathrm{DLF}}, \hat{\mathcal{X}}_{test}\rangle)},$$

where $\hat{\mathcal{X}}_{test} \in \mathbb{R}^{P^{(1)} \times P^{(2)} \times P^{(3)}}$ represents the lower-dimensional tensor obtained by applying GTDA to the tensor with respect to cerebral cortex, and $\mathcal{W}^{\mathrm{DLF}} \in \mathbb{R}^{P^{(1)} \times P^{(2)} \times P^{(3)}}$ represents regression coefficients. Next, the estimation sensitivity P_m^{se} and specificity P_m^{sp} are respectively denoted as

$$P_m^{se} = \Pr[y_{test,m} = 1|c = 1], \quad P_m^{sp} = \Pr[y_{test,m} = 0|c = 0].$$

By using each BA's estimation results $y_{i,m}$ and actual labels c_i, we respectively obtain each BA's sensitivity and specificity as follows:

$$P_m^{se} = \frac{\sum_{i=1}^{N} c_i y_{i,m}}{\sum_{i=1}^{N} c_i}, \quad P_m^{sp} = \frac{\sum_{i=1}^{N} (1 - c_i)(1 - y_{i,m})}{\sum_{i=1}^{N} (1 - c_i)},$$

where $y_{i,m}$ is obtained by the same manner shown in the previous subsection using a cross-validation scheme for the training dataset. By using $y_{i,m}$ and $\hat{\mathcal{X}}_i \in \mathbb{R}^{P^{(1)} \times P^{(2)} \times P^{(3)}}$ which is a transformed tensor obtained after GTDA with respect to cerebral cortex, the log-likelihood function of the regression coefficients $\mathcal{W}^{\mathrm{DLF}}$ of complete data is denoted as

$$\mathcal{L}(\mathcal{W}^{\mathrm{DLF}}) = \prod_{i=1}^{N} \Pr[\{y_{i,m}\}_{m=1}^{M} | \hat{\mathcal{X}}_i, \mathcal{W}^{\mathrm{DLF}}].$$

By using a set of sensitivity and specificity, the above log-likelihood function is rewritten as follows:

$$\begin{aligned}&\mathcal{L}(\mathcal{W}^{\mathrm{DLF}}) \\ &= \prod_{i=1}^{N} \Big\{\Pr[\{y_{i,m}\}_{m=1}^{M} | c_i = 1, \{P_m^{se}\}_{m=1}^{M}] \cdot \Pr[c_i = 1|\hat{\mathcal{X}}_i, \mathcal{W}^{\mathrm{DLF}}] \\ &+ \Pr[\{y_{i,m}\}_{m=1}^{M} | c_i = 0, \{P_m^{sp}\}_{m=1}^{M}] \cdot \Pr[c_i = 0|\hat{\mathcal{X}}_i, \mathcal{W}^{\mathrm{DLF}}]\Big\}.\end{aligned}$$

We assume that each BA is independent each other, $\Pr[\{y_{i,m}\}_{m=1}^{M} | c_i = 1, \{P_m^{se}\}_{m=1}^{M}]$ and $\Pr[\{y_{i,m}\}_{m=1}^{M} | c_i = 0, \{P_m^{sp}\}_{m=1}^{M}]$ can be rewritten as

$$\Pr[\{y_{i,m}\}_{m=1}^{M} | c_i = 1, \{P_m^{se}\}_{m=1}^{M}] = \prod_{m=1}^{M} [P_m^{se}]^{y_{i,m}} [1 - P_m^{se}]^{1 - y_{i,m}},$$

$$\Pr[\{y_{i,m}\}_{m=1}^{M} | c_i = 0, \{P_m^{sp}\}_{m=1}^{M}] = \prod_{m=1}^{M} [P_m^{sp}]^{1 - y_{i,m}} [1 - P_m^{sp}]^{y_{i,m}}.$$

By solving the following maximum log-likelihood problem, the optimal solution $\hat{\mathcal{W}}^{\mathrm{DLF}}$ of $\mathcal{W}^{\mathrm{DLF}}$ can be obtained

$$\hat{\mathcal{W}}^{\mathrm{DLF}} = \arg\max_{\mathcal{W}^{\mathrm{DLF}}} \mathcal{L}(\mathcal{W}^{\mathrm{DLF}}).$$

Here, the above optimization problem can be solved in the same manner as LTR (see reference [11] or Sec. **3.2**).

Given a new test data, the probabilistic label μ_c is computed as

Table 1. The details of the parameters for fMRI observation.

Name	Value
Repetition time (TR)	3000 msecs
Echo time (TE)	30.0 msecs
Flip angle (FA)	90°
Field of view (FoV)	192 mm^2
Slice thickness (Thk)	3.0 mm
Slices	36 images
Matrix size / slice	94×94 pixels
Voxel size	$2.0 \times 2.0 \times 3.0$ mm

Table 2. Number of positive/negative images.

	Positive	Negative
Subject *A*	15	25
Subject *B*	27	13
Subject *C*	18	22
Subject *D*	21	19
Subject *E*	20	20

Table 3. Accuracy of the estimated emotion.

	Comp. 1 [6]	Comp. 2	Comp. 3	Ours
Subject *A*	0.450	0.463	0.613	**0.619**
Subject *B*	0.525	0.444	0.525	**0.594**
Subject *C*	0.600	0.600	0.625	**0.644**
Subject *D*	0.475	0.638	**0.744**	0.713
Subject *E*	0.600	**0.681**	0.638	0.669
Avg.	0.530	0.565	0.629	**0.648**
Std.	0.069	0.106	0.078	**0.046**

Table 4. Relationship between comparative methods and our method. "DR" represents dimensionality reduction.

	Comp. 1 [6]	Comp. 2	Comp. 3	Ours
fMRI data	whole-brain	whole-brain	BA	BA
DR	MPCA	GTDA	MPCA	GTDA
Estimator	MI+SVM	LTR	LTR	LTR
TS-DLF	×	×	✓	✓

follows:

$$\begin{aligned}
\mu_c &= \Pr[c|\{y_{test,m}\}_{m=1}^{M}, \mathcal{X}_{test}, \mathcal{W}^{\mathrm{DLF}}] \\
&\propto \Pr[\{y_{test,m}\}_{m=1}^{M}|c, \mathcal{W}^{\mathrm{DLF}}] \cdot \Pr[c|\mathcal{X}_{test}, \mathcal{W}^{\mathrm{DLF}}] \\
&= \frac{c \cdot \gamma\rho + (1-c) \cdot \delta(1-\rho)}{\gamma\rho + \delta(1-\rho)}, \qquad (4)
\end{aligned}$$

where

$$\begin{aligned}
\rho &= \Pr[c|\hat{\mathcal{X}}_{test}, \mathcal{W}^{\mathrm{DLF}}], \\
\gamma &= \prod_{m=1}^{M} [P_m^{se}]^{y_{test,m}} [1 - P_m^{se}]^{1-y_{test,m}}, \\
\delta &= \prod_{m=1}^{M} [P_m^{sp}]^{1-y_{test,m}} [1 - P_m^{sp}]^{y_{test,m}}.
\end{aligned}$$

Finally, we can obtain the final estimation result $\hat{y}_{test}$ as

$$\hat{y}_{test} = \arg\max_{c \in \{0,1\}} \mu_c,$$

and successfully realizes the collaborative use of the multiple BA data.

The overfitting problem is solved by dividing whole-brain data into the multiple BA data and integrating of the LTR-based estimation results. Moreover, TS-DLF can consider the LTR-based estimators' sensitivity and specificity shown in Eq. (4) to accurately integrate these estimation results.

4. EXPERIMENTAL RESULTS

This section presents the experimental results to verify the effectiveness of our method. First, we explain an image dataset used for the visual stimuli. In this experiment, we utilized *Affective Image Classification Dataset* [20]. This dataset consists of 807 images, and each image has one of the eight emotional categories. Specifically, these categories are *Amusement*, *Awe*, *Contentment*, *Excitement* as "positive" emotions and *Anger*, *Disgust*, *Fear*, *Sad* as "negative" emotions. We randomly selected five images for each of the eight categories and used total 40 images as the image dataset.

In this experiment, five healthy subjects, named Subject *A*, Subject *B*, . . . , Subject *E* (average 26 years old) participated. The fMRI data were captured with the 3T MRI scanner (Siemens MAGNETOM Prisma[2]). Table 1 shows the parameters for the fMRI observation. We dealt with block design (task: watching an image for 12 secs, rest: resting-state for 12 secs). Since we obtained 4 samples per block, the number of the obtained fMRI data were 160 (= 40×4). Furthermore, all subjects evaluated each image by an emotional category that fall under any of the eight categories, and the categories were grouped into the two classes, *i.e.,* "positive" ($c = 1$) and "negative" ($c = 0$). In this experiment, these classes were used as the ground truth, and Table 2 shows the number of positive and negative images with respect to each subject. The verification method was five fold cross-validation.

Results of our experiment are shown in Table 3. In this table, we also show the results of three comparative methods shown in Table 4. The improvement of the estimation accuracy for most subjects and the average can be confirmed by the results in Table 3. The results of Comp. 2 and Ours show the effectiveness of obtaining multiple BA data and integration of these estimation results. The results of Comp. 3 and Ours show the effectiveness of applying supervised tensor dimensionality reduction, GTDA. Moreover, Ours outperforms the *state-of-the-art* approach [6], *i.e.,* Comp. 1, that applies multilinear principal component analysis (MPCA) [21] to whole-brain data, feature selection based on mutual information (MI) and SVM-based estimation. Therefore, the results show the effectiveness of our method.

5. CONCLUSION

In this paper, we have presented a novel method for estimating human emotion evoked by visual stimuli using fMRI data. We divide whole-brain fMRI data according to the BAs, and then apply GTDA and LTR to the BA data. These procedures solve the problem of the overfitting. Finally, the integration of the multiple estimation results based on TS-DLF enables the collaborative use of the multiple BAs' results. Consequently, our method has realized the improvement of the estimation performance.

[2]http://www.siemens.com/

6. REFERENCES

[1] C. Mühl, B. Allison, A. Nijholt, and G. Chanel, "A survey of affective brain computer interfaces: principles, state-of-the-art, and challenges," *Brain-Computer Interfaces*, vol. 1, no. 2, pp. 66–84, 2014.

[2] R. W. Picard, *Affective computing*. MIT Press Cambridge, 1997.

[3] D. D. Cox and R. L. Savoy, "Functional magnetic resonance imaging (fMRI) "brain reading": detecting and classifying distributed patterns of fMRI activity in human visual cortex," *Neuroimage*, vol. 19, no. 2, pp. 261–270, 2003.

[4] K. A. Norman, S. M. Polyn, G. J. Detre, and J. V. Haxby, "Beyond mind-reading: multi-voxel pattern analysis of fMRI data," *Trends in Cognitive Sciences*, vol. 10, no. 9, pp. 424–430, 2006.

[5] F. Pereira, T. Mitchell, and M. Botvinick, "Machine learning classifiers and fMRI: a tutorial overview," *Neuroimage*, vol. 45, no. 1, pp. S199–S209, 2009.

[6] X. Song, L. Meng, Q. Shi, and H. Lu, "Learning tensor-based features for whole-brain fMRI classification," in *Proceedings of International Conference on Medical Image Computing and Computer-Assisted Intervention*, 2015, pp. 613–620.

[7] O. Yamashita, M. Sato, T. Yoshioka, F. Tong, and Y. Kamitani, "Sparse estimation automatically selects voxels relevant for the decoding of fMRI activity patterns," *NeuroImage*, vol. 42, no. 4, pp. 1414–1429, 2008.

[8] S. Ryali, K. Supekar, D. A. Abrams, and V. Menon, "Sparse logistic regression for whole-brain classification of fMRI data," *NeuroImage*, vol. 51, no. 2, pp. 752–764, 2010.

[9] K. Brodmann, *Vergleichende Lokalisationslehre der Grosshirnrinde in ihren Prinzipien dargestellt auf Grund des Zellenbaues*. Barth, 1909.

[10] D. Tao, X. Li, X. Wu, and S. J. Maybank, "General tensor discriminant analysis and gabor features for gait recognition," *IEEE Transaction on Pattern Analysis and Machine Intelligence*, vol. 29, no. 10, pp. 1700–1715, 2007.

[11] X. Tan, Y. Zhang, S. Tang, J. Shao, F. Wu, and Y. Zhuang, "Logistic tensor regression for classification," in *Proceedings of International Conference on Intelligent Science and Intelligent Data Engineering*. Springer, 2012, pp. 573–581.

[12] C. Cortes and V. Vapnik, "Support-vector networks," *Machine Learning*, vol. 20, pp. 273 –297, 1995.

[13] V. C. Raykar, S. Yu, L. H. Zhao, G. H. Valadez, C. Florin, L. Bogoni, and L. Moy, "Learning from crowds," *Journal of Machine Learning Research*, vol. 11, no. 7, pp. 1297–1322, 2010.

[14] C. Khatri and C. R. Rao, "Solutions to some functional equations and their applications to characterization of probability distributions," *Sankhyā: The Indian Journal of Statistics, Series A*, pp. 167–180, 1968.

[15] J. D. Carroll and J. Chang, "Analysis of individual differences in multidimensional scaling via an N-way generalization of "Eckart-Young" decomposition," *Psychometrika*, vol. 35, no. 3, pp. 283–319, 1970.

[16] R. A. Harshman, "Foundations of the parafac procedure: Models and conditions for an "explanatory" multi-modal factor analysis," *UCLA Working Papers in Phonetics*, vol. 16, pp. 1–84, 1970.

[17] J. A. Maldjian, P. J. Laurienti, R. A. Kraft, and J. H. Burdette, "An automated method for neuroanatomic and cytoarchitectonic atlas-based interrogation of fMRI data sets," *Neuroimage*, vol. 19, no. 3, pp. 1233–1239, 2003.

[18] J. A. Maldjian, P. J. Laurienti, and J. H. Burdette, "Precentral gyrus discrepancy in electronic versions of the talairach atlas," *Neuroimage*, vol. 21, no. 1, pp. 450–455, 2004.

[19] K. J. Friston, J. T. Ashburner, S. J. Kiebel, T. E. Nichols, and W. D. Penny, *Statistical parametric mapping: the analysis of functional brain images: the analysis of functional brain images*. Academic press, 2011.

[20] J. Machajdik and A. Hanbury, "Affective image classification using features inspired by psychology and art theory," in *Proceedings of the ACM International Conference on Multimedia*, 2010, pp. 83–92.

[21] H. Lu, K. N. Plataniotis, and A. N. Venetsanopoulos, "MPCA: Multilinear principal component analysis of tensor objects," *IEEE Transaction on Neural Networks*, vol. 19, no. 1, pp. 18–39, 2008.